Polymer Bulletin 58, 541–551 (2007)
DOI 10.1007/s00289-006-0692-2

Polymer Bulletin

Effect of temperatures in the rearmost stabilization zone on structure and properties of PAN-based oxidized fibers

Min Jing[1,2] (✉), Cheng-guo Wang[2] (✉), Yu-jun Bai[2], Bo Zhu[2], Yan-xiang Wang[2]

[1]Key Laboratory of Liquid Structure and Heredity of Materials, Ministry of Education, Shandong University, Jinan 250061, China
[2]Carbon Fiber Engineering Research Center of Shandong Province, College of Materials Science and Engineering, Shandong University, Jinan 250061, China

Received: 10 June 2006 / Revised version: 29 September 2006 / Accepted: 5 October 2006
Published online: 13 October 2006 –

Summary

Temperature in the rearmost stabilization zone has an important impact on the final stabilization degree of PAN precursor fibers during industrial successive pre-oxidation and on their structure and properties. FTIR, X-ray diffraction, elemental analysis, ultramicrotomy and optical microscopy were used to study the slow evolution of stabilization indices and structure changes with increasing the temperature in the rearmost zone. The results show that cross linking reaction happens above 240°C in the rearmost stabilization zone, leading to a quick increase of oxygen content and aromatization index and the formation of cross-linking rigid structure. Especially for the sample treated at 275°C, the cross-linking structure induces a compact sheath layer in the fiber which impedes the oxygen atoms diffusion inward. By changing the temperature in the rearmost stabilization zone, the oxygen content, chemical structure and aromatization index can be accurately controlled.

Introduction

As has been known, polyacrylonitrile (PAN)-based carbon fibers as strengthened materials of composites are now applied in many fields. The conversion from PAN solution to high-strength carbon fiber contains three key stages: spinning, stabilization and carbonization, and the stabilization of precursor fibers is a very important process because the mechanical properties of the ultimate carbon fiber depend greatly upon the quality of oxidized fiber [1-4]. Modern stabilization method is to pass the precursor tow continuously through a furnace divided into several zones with increasing temperature gradient for the purpose of low cost and high efficiency [3]. Many aspects during stabilization including physical and chemical changes [5-12], micro- and macro- structure and properties [13-18] of oxidized fibers have been studied in the past decades and some optimum stabilization indices were suggested, such as oxygen content, aromatization index, the avoidance of skin-core structure and proper heating rate, time, temperature and so on [3,9,17,19-21].

During successive stabilization, temperature above 250°C has more obvious influence on the oxidized fibers than that at initial stage. Mathur [22] considered that thermal stabilization of PAN fibers is not at all complete even at 300°C. So he studied the

structure and properties of the samples stabilized at higher temperature about 300~400°C. But Jain's review [4] pointed out that temperature higher than 300°C could cause violent exothermic reactions resulting in significant weight loss. Some investigators [4,19,23,24] favored that the oxygen content in oxidized fibers for carbon fiber should be controlled within the range of 8~12%. In this work, a kind of PAN fiber wet-spun using a copolymer of polyacrylonitrile/ammonium itaconate was stabilized continuously through increasing temperature zones. The structure and properties of oxidized fibers and the effect of temperature in the rearmost stabilization zone were investigated. To our surprise, some information was obtained, which is helpful for optimizing pre-oxidation technology.

Experimental

Preparation of precursor fibers

A free-radical copolymerization of 99.4 wt.% acrylonitirle and 0.6 wt.% ammonium itaconate [$IA(NH_4)_2$] was initiated by azodiisobutyronitrile (AIBN) in dimethylsulfoxide (DMSO). The spinning solution consists of 23% copolymer with an average molecular weight of about 1.4×10^5. The dope was wet-spun into precursor fiber with each single tow containing 1000 filaments, and a single filament has quality indices of 1.06 dtex in titer, 8.77 MPa in tensile strength and 9.7% in elongation.

Stabilization and carbonization

Figure 1 shows two self-designed oxidizing furnaces used for stabilization in air. Each oxidizing furnace has five temperature zones with 2.4 m in length which are heated by purified hot air flow and electric resistance wires. The temperatures are controlled by a computer. PAN fiber may continuously pass through the oxidizing furnaces at an initial feeding speed of 0.3m/min. The stretch ratio between A and B is 3% and between B and C is 5% while between C and F is zero. In our experiments, the temperatures designated to the 9 zones are 196, 206, 221, 231, 241, 246, 250, 261, and 268°C, respectively. The fibers from zone 9 were subjected to various treatments in the rearmost stabilization zone 10 at temperatures of 210, 230, 240, 250, 260 and 275°C, respectively. The sample codes of the oxidized fibers obtained from the above experiments are listed in Table 1.

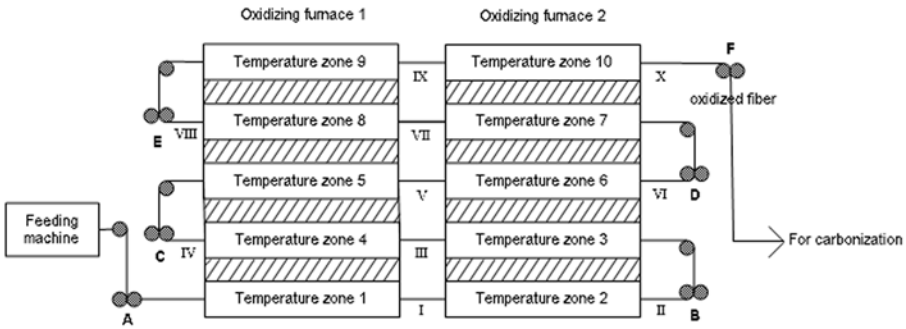

Figure 1. Scheme of stabilization and carbonization line. A-H: driving wheel of the equipment; I-X: sampling site

Table 1. Sample codes of the oxidized fibers obtained from stabilization experiments

Sample code	Temp. zone	Temp. (°C)	Site in Figure 1
P	/	25	Precursor fiber
S1	1	196	I
S2	2	206	II
S3	3	221	III
S4	4	231	IV
S5	5	241	V
S6	6	246	VI
S7	7	250	VII
S8	8	261	VIII
S9	9	268	IX
S10-1	10	210	X
S10-2	10	230	X
S10-3	10	240	X
S10-4	10	250	X
S10-5	10	260	X
S10-6	10	275	X

Characterization

The titer of single precursor filament was determined by a XD-1 fiber fineness machine, and the tensile strength and elongation of the precursor and oxidized fibers was determined by a XQ-1 tensile testing machine. Both the machines were made in Donghua University, Shanghai, China. The density of fibers was obtained at 25°C by a sink/float method in a mixture of n-heptane and carbon tetrachloride. Differential scanning calorimetry (DSC) was performed on a German NETZSCH404 thermal analyzer. After drying and chopping, 2mg PAN fiber sample was heated at a rate of 10°C•min^{-1} in air. Mass percent contents of oxygen (O), nitrogen (N), carbon (C) and hydrogen (H) elements were obtained by a German GmbH Vario EL III elemental analyzer. About 2 mg samples of precursor fibers or oxidized fibers were chopped into tiny fuzz and packed into small tin boats. Oxygen element analysis was achieved by heating the samples to 1150°C in argon atmosphere, while N, C, H element analysis was performed at 950°C in oxygen using argon as carrier gas. Fourier transform infrared (FT-IR) measurement was conducted on an American Bruker Vector 22 spectrometer using KBr disks pressed by mixing 2 mg sample of precursor fibers or oxidized fibers with 200 mg KBr. A Rigaku D/max-rc X-ray diffractometer with Ni-filtered CuK_α radiation (the wavelength λ=0.1541 nm) was used to determine the structure of fibers with an accelerated voltage of 40 kV and a current of 60 mA, a scanning rate of 3°/min and a scanning step of 0.02°. Scherrer formula was used to calculate the crystallite size L_c:

$$L_c = \frac{K\lambda}{B\cos\theta} \qquad (\mathbf{1})$$

where λ is the wavelength of CuK_α radiation, θ is the Bragg angle, B is the full width at half the maximum intensity (FWHM) of the (100) peak around 2θ = 17.0°, and K is a constant, assigned as 0.89. A tow of oxidized fibers was embedded in epoxy resin and solidified before cutting. Transverse ultrathin sections of 0.7 μm in thickness were cut by a Reichert-Jung ultramicrotome. The ultrathin sections were observed in a JXA-840 optical microscope (OM) with a camera.

Results and discussion

Thermal analysis of precursor fibers

Figure 2 gives the differential scanning calorimetry (DSC) curve of PAN fiber specimen P heated in air. Two exothermic peaks can be distinguished in the temperature range of 221.6-380.2°C. The obvious peak around 288.1°C implies that cyclization reaction initiates at 221.6°C and culminates at 288.1°C. The inflection point at 305.1°C is likely related to oxygen incorporation or oxidation [10].

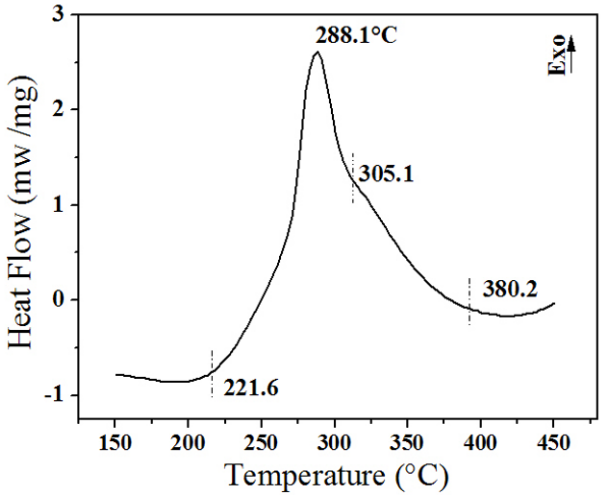

Figure 2. The differential scanning calorimetry (DSC) curve of precursor fiber specimen P in air

Changes in XRD structure

Figure 3 and 4 show the X-ray diffraction (XRD) patterns of some oxidized fibers and the corresponding precursor fiber. Two peaks occur at 2θ=17 and 29.5° in the XRD pattern of PAN precursor fiber. During stabilization, the intensity of these two peaks is slightly strengthened below 231°C. This is because the dominant chemical reaction in the DSC curve shown in Figure 1 has not happened at such low temperature, but the crystallinity and orientation in the fibers increase owing to stretching and heating. When the fibers were heated to higher temperatures, the structures begin to transform due to the occurrence of chemical reactions such as cyclization and dehydrogenation. The peaks at 2θ=17.0 and 29.5° weaken gradually and broaden, demonstrating a decrease in crystal size and crystallinity. Simultaneously, a new wide and flat peak appears at 2θ=25.5° [20]. This can be confirmed by the data in Table 2.
The aromatization index (A.I.) during stabilization can be calculated by the following formula [20]:

$$A.I. = \frac{I_A}{I_A + I_P} \tag{2}$$

where I_A is the diffraction intensity of the aromatic structure around 2θ=25°, and I_P is the diffraction intensity of the peak around 2θ=17°. The A.I. values of oxidized fibers in the rearmost stabilization zone are also listed in Table 3.

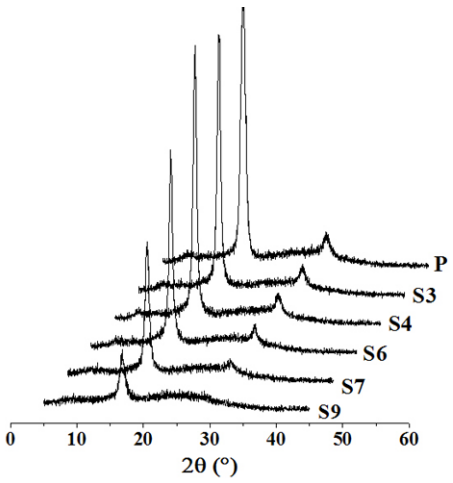

Figure 3. XRD patterns of oxidized fibers and the corresponding PAN precursor fibers

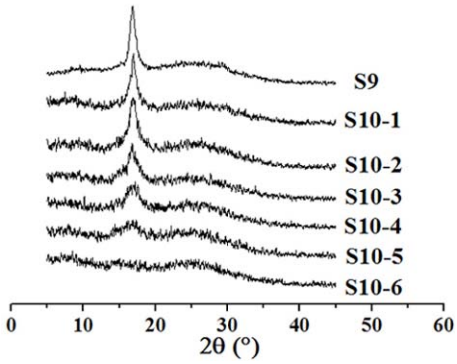

Figure 4. XRD patterns of oxidized fiber obtained from temperature zones 9 and 10

Table 2. Data obtained from the XRD patterns in Figure 3

Sample code	2θ=17° peak FWHM (°)	2θ=17° peak intensity (CPS)	Average Lc (nm)
P	0.876	3129	9.07
S3	0.611	3025	13.00
S4	0.557	3250	14.26
S6	0.579	2311	13.72
S7	0.684	1555	11.62
S9	0.772	624	10.29

Table 3. Data obtained from the XRD patterns in Figure 4

Sample code	2θ=17° peak FWHM (°)	Average Lc (nm)	Aromatization Index (%)
S9	0.772	10.29	18.69
S10-1	0.835	9.51	25.06
S10-2	1.035	7.68	27.73
S10-3	1.22	6.51	33.50
S10-4	1.507	5.27	38.72
S10-5	2.235	3.55	51.30
S10-6	/	/	64.44

In the rearmost stabilization zone, the peak around 2θ=17° continues to weaken with the increase of temperature, as show in Figure 4. However, the peak around 2θ=25.5°

strengthens gradually as a result of the increment of A.I. values. The peak around 2θ=17° nearly completely disappears, and the FWHM and average *Lc* cannot be determined in XRD pattern of S10-6. But the A.I. value of S10-6 reaches up to 64.44%. The diffraction peak around 2θ=17° reflects the crystal region made up of PAN linear macromolecules and the peak around 2θ=25.5° relates to the ladder polymer structure. The transformation from the former structure to the latter one can be seen from the XRD patterns in Figure 4, where the heating temperature plays a significant role in the transformation.

Changes in chemical structure

The IR spectra of samples from the stabilization zones 1 to 9 are shown in Figure 5. Some noticeable changes in IR spectra during oxidization have been studied in many papers [7-9,13,22]. The peak at 2240 cm^{-1} (C≡N stretching vibration) as well as peaks at 2939 cm^{-1} (CH_2 stretching vibration), 1456 cm^{-1} (CH_2 bending vibration), 1356 cm^{-1} (CH in-plane-bending), 1255 cm^{-1} (CH_2 wagging) and 1070 cm^{-1} (C－CN stretching vibration) abruptly decrease, reflecting the disappearance of linear structure due to cyclization and dehydrogenation reaction. Some new peaks appear at about 1645 cm^{-1} and 1543 cm^{-1}. At the same time the intensity of the peak at 1700~1000 cm^{-1} bands increases due to the overlapping of frequencies of different modes vibration (possibly conjugated C=C, C=N, C=O, and NH associated with heteroatomic ring systems). These show that various and complicated chemical structures produce with the progress of oxidation.

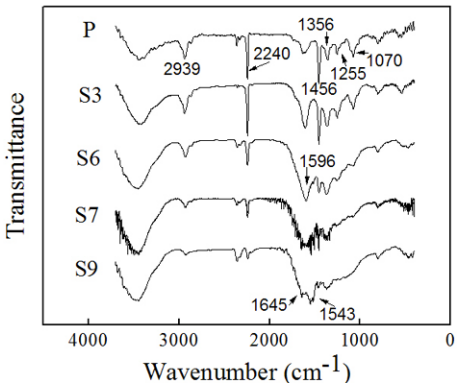

Figure 5. FT-IR spectra of the precursor fiber and the oxidized fiber obtained from zones 1 to 9

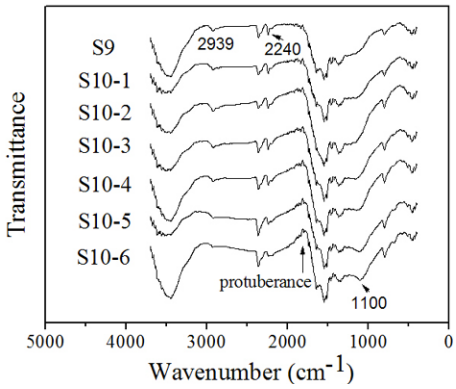

Figure 6. FT-IR spectra of the oxidized fibers in the rearmost stabilization zone with different heating treatment temperature

Figure 6 is the FT-IR spectra of the oxidized fibers from the rearmost stabilization zone with different heating treatment temperatures. With raising the temperature, the intensity of bands at 2240 cm^{-1} and 2939 cm^{-1} continue to decrease gradually and the spectra at 1700-1000 cm^{-1} continue to broaden and strengthen. Few linear C≡N and CH_2 group left in the spectra of sample S10-6 at last. These facts indicate that temperature plays an important role in the cyclization and dehydrogenation reaction.

For the oxidized fibers treated below 275°C in the rearmost stabilization zone 10, cyclization reaction and the formation of ladder structure are not complete.

It is very interesting that there are two new changes appearing in Figure 6. One is a low and wide peak at 1100 cm^{-1}, an indication that C—O—C group [19] increases during cross-linking by chemically bound oxygen. It is worth the whistle that the temperatures applied to samples S10-4 and S10-5 are lower than the temperature to S9, but the peak at 1100 cm^{-1} in the former spectra is more visible than that in the latter one. This verifies the viewpoint from Bashir [11] that the presence of a cyclized polymer is necessary for oxygen incorporation on the back bone structure. The other change is that an upward protuberance near 1800 cm^{-1} as a result of the transmittance of the fibers poorer and poorer in durative oxidation process. The protuberance does not come into being in the IR spectrum of sample S9 but starts to form in the spectrum of sample S10-1 and becomes sharper and sharper with the increase of temperature.

Chemical reactions also result in the changes of elemental compositions. The elemental contents at various stages are listed in Table 4. The decrease of molar ratio of N/C and H/C in pre-oxidation process owns to the cyclization reaction, dehydrogenation reaction. Oxidation reaction causes an increase in oxygen content, and the higher the temperature is in the rearmost stabilization zone, the higher the oxygen content is. Although the oxygen contents in samples S10-2~S10-6 are all in the optimum range of 8~12% [4,19,23,24], the chemical structures and phase structures of these samples have changed greatly as seen in Figure 6 and 4. By changing the temperature in the rearmost stabilization zone, oxygen content, chemical structure and aromatization index can be accurately controlled, which can be employed to optimize pre-oxidation technology.

Table 4. Results of elemental analysis on precursor fiber and oxidized fibers

Sample code	Wt% of element O (%)	Molar C	Molar N	Molar H	Molar O
Precursor	2.665	12	3.92	12.36	0.22
S1	2.494	12	3.90	12.35	0.20
S3	3.058	12	3.89	12.01	0.29
S6	4.599	12	3.89	11.63	0.53
S7	5.160	12	3.86	11.45	0.61
S9	7.625	12	3.80	10.49	0.98
S10-1	7.750	12	3.80	10.45	0.99
S10-2	8.166	12	3.78	10.12	1.08
S10-3	8.715	12	3.76	10.05	1.16
S10-4	9.477	12	3.77	10.00	1.32
S10-5	10.23	12	3.75	9.80	1.35
S10-6	11.76	12	3.70	9.31	1.64

Note: The molar values are normalized by taking 12 moles of carbon for comparison as Mathur [22] does.

Changes in properties

Structure determines properties. From the aforementioned FT-IR spectra and XRD patterns, the substitution of ladder structure in sample S9 for the majority of PAN

linear macromolecules in precursor fiber promotes the thermal stability of S9. Figure 7 shows the properties of oxidized fibers as a function of treatment temperature. With increasing the temperature in the rearmost stabilization zone, the changes of density and tensile strength of samples (curve 1 and 4) are not as dramatic as those in zones 1-9 (curve 2 and 3). So, temperature has less impact on the density and tensile strength of sample with ladder structure. In the rearmost stabilization zone, the density increase is partially due to the cyclization of residual PAN linear macromolecular and mostly due to the cross-linking reaction.

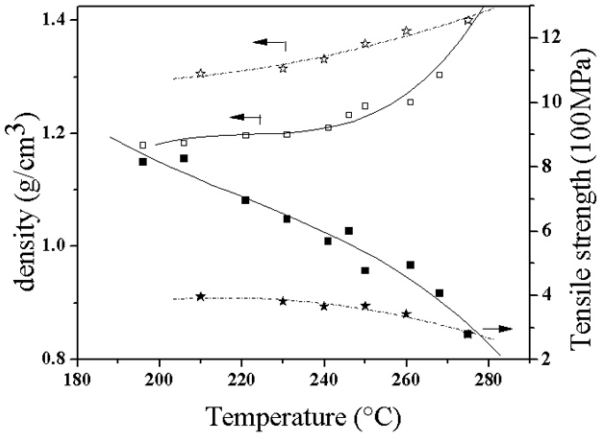

Figure 7. Properties of oxidized fibers as a function of treatment temperature. Curve 1: density changes with the increase of temperature in the rearmost stabilization zone; Curve 2: density changes from stabilization zone 1 to 9; Curve 3: tensile strength changes from stabilization zones 1 to 9; Curve 4: tensile strength changes with the increase of temperature in the rearmost zone

Changes in cross-section morphology structure

Transverse ultrathin sections cut from samples S9, S10-2, S10-4 and S10-6 were observed by optical microscope as shown in Figure 8. It can be seen that, the diameter of the fiber becomes smaller with the increase of heating temperature due to the shrinkage along radial direction induced by intermolecular cross-linking reaction. At the same time, the cross-sections of samples S9 and S10-2 are not as regular as those of others. This can be explained that these fibers are soft and have good tenacity, some deformation may happen during cutting the samples.

Three different skin-core morphologies can be observed in Figure 8b, c and d and for the convenience of comparison, some typical cross-sections of single filament were placed together, as displayed in Figure 9. The first line shows kidney-shaped cross-sections and the second line shows circle shape. These two kinds of cross-section shape in a tow oxidized fibers form in spinning process related to the spinning conditions. Some other information about the four samples is listed in Table 5. Compare with sample S9, only the A.I. value and density of sample S10-2 slightly increase, and the cross-section morphology is almost similar to that of S9,

they are comprised of cyclized ladder structure in skin and incompletely cyclized PAN molecular in core. But the skin-core structure of fiber S10-4 and S10-6 are different from the former two. At temperatures over 240°C, many oxygen atoms incorporate into the fiber chemical structure to act as bridges between the adjacent molecular chains, producing a rigid structure. So the cross-section morphology of S10-4 and S10-6 is regular. This cross-linking structure forms on the surface of oxidized fiber at first and then pushes inward. The sheath of sample S10-4 has this cross-linking structure in skin but not in the core and the interface of the two zones is not very obvious. However, the two-zone boundary of sample S10-6 is clear. We speculate that at 275°C the diffusion rate of oxygen atom from the surface to the inner of a filament is slower than the cross-linking reaction rate, so many oxygen atoms are settled in the sheath of S10-6 to form a cross-linking compact layer which slows up the inward diffusion of oxygen atoms and impedes oxygen into the core portion [25-27]. Oxygen atoms concentrate in the skin of S10-6 thereby the skin-core boundary is distinct.

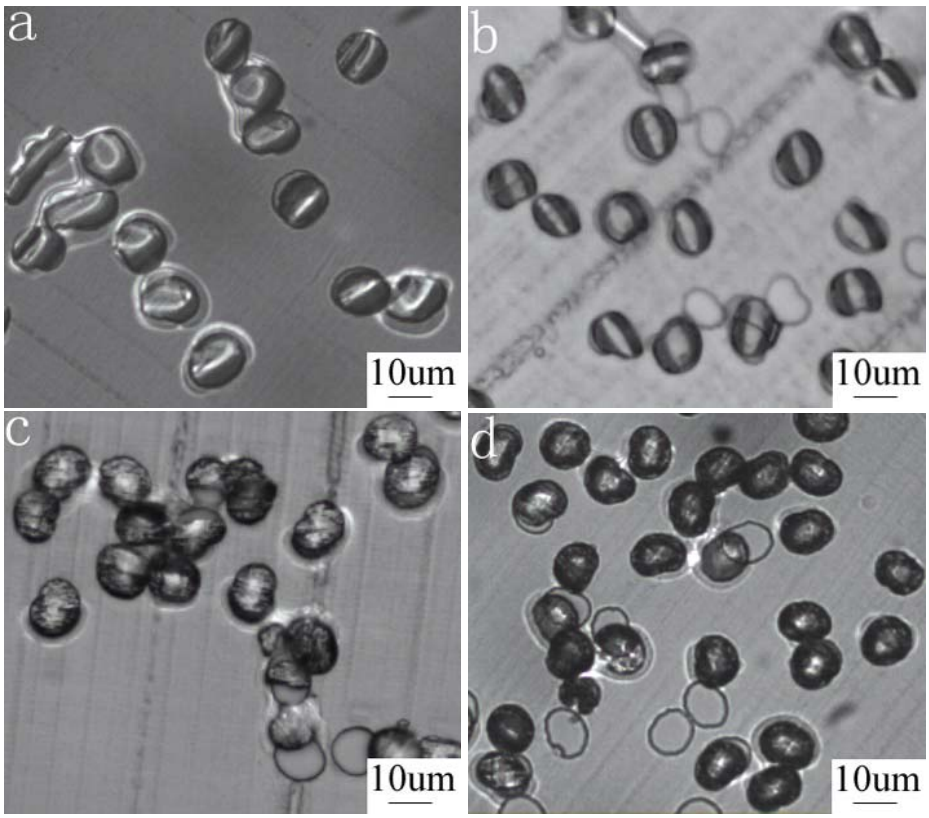

Figure 8. OM photographs of transverse ultrathin sections of some oxidized fibers treated at different temperatures. (a) S9 (b) S10-2 (c) S10-4 (d) S10-6

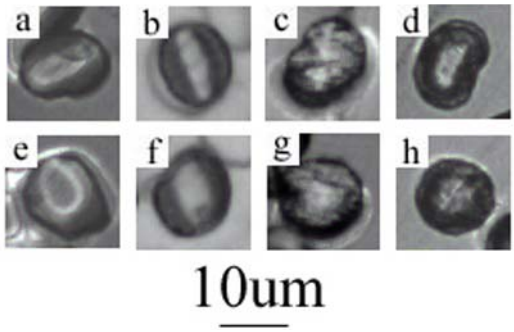

Figure 9. Comparison of magnified OM photographs of transverse ultrathin sections from single filament. (a)~(d): kidney-shaped cross-sections; (e)~(h): circular shape cross-sections; (a) and (e): S9; (b) and (f): S10-1; (c) and (g): S10-4; (d) and (h): S10-6

Table 5. Comparison of four samples on structure and property

Sample code	Wt% of O (%)	O:C	H:C	C─O peak in IR	C≡N peak in IR	Aromatization Index (%)	Density (g/cm^3)
S9	7.625	0.98:12	10.49:12	no	small	18.54	1.304
S10-2	8.166	1.08:12	10.12:12	no	small	27.73	1.315
S10-4	9.477	1.32:12	10.00:12	a little	smaller	38.72	1.358
S10-6	11.76	1.64:12	9.31:12	protuberant	few	64.44	1.400

Conclusions

By characterizing the structure and properties of oxidized fibers treated at different temperatures in the rearmost stabilization zone, some evolution including the transformation of two phase structure, the increase of aromatization index, the gradual formation of cross-linking structure and the changes of cross-section morphology can be detected, from which the following conclusion can be drawn:

(1) At temperature below 230°C, the changes of structure and properties is not obvious. But when the temperature is above 240°C, the occurrence of cross-linking reaction leads to a quick increase in oxygen content and aromatization index and to the formation of cross-linking rigid structure.

(2) The formation of cross-linking structure in sheath makes the cross-section morphology of samples treated above 240°C in the rearmost stabilization zone different from those treated below 230°C. When the sample is treated at 275°C, a cross-linking compact layer in the sheath will impede the diffusion of oxygen atoms inward.

(3) By changing the temperature in the rearmost stabilization zone, oxygen content, chemical structure and aromatization index can be accurately controlled, which can be employed to optimize pre-oxidation technology.

Acknowledgements. The author acknowledges financial support from National Natural Science Foundation of China, grant number 50673052.

References

1. Fitzer E, Heym M (1976) Chemistry and Industry 21:663
2. Morita K, Miyachi H, Hiramatsu T (1981) Carbon 19:11
3. Walsh PJ (2001) ASM Handbook 21:35
4. Jain MK, Abhiraman AS (1987) J Mater Sci 22:278
5. Usaml T, Itoh T, Ohtani H, Tsuge S (1990) Macromolecules 23:2460
6. Boccara AC, Fournier D, Kumar A, Pandey GC (1997) J Appl Polym Sci 63:1785
7. Coleman MM, Sivy G.T (1981) Carbon 19:123
8. Varma SP, Lal BB, Srivastava NK (1976) Carbon 14:207
9. Rašković V, Marinković S (1975) Carbon 13:535
10. Sen K, Bajaj P, Sreekumar TV (2003) J Polym Sci Pol Phy 41:2949
11. Bashir Z (1991) Carbon 29:1081
12. Wu G, Lu C, Ling L, Hao A, He F (2005) J Appl Polym Sci 96:1029
13. Zhang W, Liu J, Wu G (2003) Carbon 41:2805
14. Deurberoue A, Oberlin A (1991) Carbon 29:621
15. KO T, Lin C (1989) J Appl Polym Sci 37:553
16. Dalton S, Heatley F, Budd PM (1999) Polymer 40:5531
17. Ko T, Ting H, Lin C (1988) J Appl Polym Sci 35:631
18. Mochida I, Zeng S, Korai Y, Toshima H (1990) Carbon 28:193
19. Ogawa H, Saito K (1995) Carbon 33:783
20. Bahl OP, Manocha LM (1974) Carbon 12:417
21. Uchida T, Shinoyama I, Ito Y, Nukuda K (1971) Proc 10th Biennial Carbon Conf, Am Carbon Soc:31
22. Mathur RB, Bahl OP, Mittal J (1992) Carbon 30:657
23. Toho Beslon Co Ltd (1978) US Patent 4069297
24. Gupta AK, Paliwal DK, Bajaj P (1991) J Macromol Sci Rev Macromol Chem Phys C31:1
25. Matsumoto T, Mochida I (1993) Carbon 30:143
26. Blanco C, Lu S, Appleyard SP, Rand B (2003) Carbon 41:165
27. Warner SB, Peebles LH, Uhlmann DR (1979) J of Mater Sci 14:556